EXPERIMENTAL CELL RESEARCH 315 (2009) 3052–3063

available at www.sciencedirect.com

ScienceDirect

www.elsevier.com/locate/yexcr

Research Article

Dynamic clustering and dispersion of lipid rafts contribute to fusion competence of myogenic cells

Atsushi Mukai[a], *Tomohiro Kurisaki*[b], *Satoshi B. Sato*[c], *Toshihide Kobayashi*[d], *Gen Kondoh*[e], *Naohiro Hashimoto*[a,*]

[a]*Department of Regenerative Medicine, National Institute for Longevity Sciences, National Center for Geriatrics and Gerontology, 36-3 Gengo, Morioka, Oobu, Aichi 474-8522, Japan*
[b]*Department of Growth Regulation, Institute for Frontier Medical Sciences, Kyoto University, 53 Shogoin-Kawahara-cho, Sakyo-ku, Kyoto 606-8507, Japan*
[c]*Research Center for Low Temperature and Material Sciences, Kyoto University, Yoshida-honmachi, Kyoto 606-8501, Japan*
[d]*Lipid Biology Laboratory, Discovery Research Institute, RIKEN, Wako, Saitama 351-0198, Japan*
[e]*Laboratory of Animal Experiments for Regeneration, Institute for Frontier Medical Sciences, Kyoto University, 53 Shogoin-Kawahara-cho, Sakyo-ku, Kyoto 606-8507, Japan*

ARTICLE INFORMATION

Article Chronology:
Received 31 March 2009
Revised version received 22 June 2009
Accepted 8 July 2009
Available online 14 July 2009

Keywords:
Myogenesis
Cell fusion
Lipid raft
M-cadherin
Myoblast
Membrane cholesterol

ABSTRACT

Recent research indicates that the leading edge of lamellipodia of myogenic cells (myoblasts and myotubes) contains presumptive fusion sites, yet the mechanisms that render the plasma membrane fusion-competent remain largely unknown. Here we show that dynamic clustering and dispersion of lipid rafts contribute to both cell adhesion and plasma membrane union during myogenic cell fusion. Adhesion-complex proteins including M-cadherin, β-catenin, and p120-catenin accumulated at the leading edge of lamellipodia, which contains the presumptive fusion sites of the plasma membrane, in a lipid raft-dependent fashion prior to cell contact. In addition, disruption of lipid rafts by cholesterol depletion directly prevented the membrane union of myogenic cell fusion. Time-lapse recording showed that lipid rafts were laterally dispersed from the center of the lamellipodia prior to membrane fusion. Adhesion proteins that had accumulated at lipid rafts were also removed from the presumptive fusion sites when lipid rafts were laterally dispersed. The resultant lipid raft- and adhesion complex-free area at the leading edge fused with the opposing plasma membrane. These results demonstrate a key role for dynamic clustering/dispersion of lipid rafts in establishing fusion-competent sites of the myogenic cell membrane, providing a novel mechanistic insight into the regulation of myogenic cell fusion.

Introduction

Skeletal muscle fibers are multinucleated cells that are derived from multinucleated myotubes. This muscle-specific syncytium is formed by the fusion of mononucleated myogenic progenitor cells (myoblasts) that are descendants of muscle stem cells called muscle satellite cells. Myoblasts show unique capacities, including multipotentiality [1] and the ability to fuse with each other or to existing myofibers in a cell-autonomous way during both postnatal growth and repair of skeletal muscle. Myoblast fusion consists of a

* *Corresponding author.*
E-mail address: nao@nils.go.jp (N. Hashimoto).
Abbreviations: CTB, cholera toxin B subunit; fPEG-Chol, fluorescein-labeled poly(ethylene glycol) cholesteryl ester; MCD, methyl-β-cyclodextrin

0014-4827/$ – see front matter © 2009 Elsevier Inc. All rights reserved.
doi:10.1016/j.yexcr.2009.07.010

series of steps: myoblast–myoblast contact, recognition, adhesion, and plasma membrane breakdown/union [2–4]. Each step of myoblast fusion is strictly regulated at cellular and subcellular levels. Plasma membrane breakdown/union is initially induced in a discrete area of the plasma membrane [5,6]. Thus, these studies imply specialization of presumptive fusion sites in the plasma membrane of myogenic cells.

The molecular mechanisms that control each step of myogenic cell fusion remain to be resolved, although a number of molecules have been implicated in regulating muscle fiber formation. Extracellular matrix receptor integrins and adhesion molecules such as cadherins, NCAM, CD9, CD81, and ADAMs may contribute to the regulation of the recognition/adhesion steps of myoblast fusion [7–9]. However, how they coordinate their functions in the recognition/adhesion steps at the discrete, presumptively fusion-competent site of the plasma membrane remains to be determined. In addition, it remains puzzling what molecular events trigger plasma membrane breakdown/union at the presumptively fusion-competent site after establishing the cell adhesion that is prerequisite for plasma membrane union.

Cholesterol is involved in maintaining membrane fluidity and the structure of lipid microdomains/rafts. The concentration of membrane cholesterol in myoblasts decreases prior to membrane fusion because an increase of membrane fluidity is required for plasma membrane union [10]. In fact, membrane fusion takes place within the cholesterol-free sites of the myoblast plasma membrane [11]. Furthermore, preventing membrane cholesterol levels from declining inhibits myoblast fusion [12]. Therefore, while cholesterol has been implicated in membrane fusion of myoblasts [12,13], the molecular mechanisms that regulate redistribution of membrane cholesterol at the presumptively fusion-competent sites of the plasma membrane remain to be identified.

Our previous study showed that the leading edge of lamellipodia of myogenic cells contain a fusion-competent site of plasma membrane [5]. To identify the key molecules that render the plasma membrane of lamellipodia fusion-competent, we determined a stimulus that enhances muscle cell fusion in vitro. We found that cholera toxin B subunit (CTB), which binds to ganglioside GM1 localized in lipid rafts/microdomains, enhanced muscle cell fusion. Furthermore, our data suggest a pivotal role for lipid rafts in both accumulation of adhesion molecules and redistribution of membrane cholesterol at the presumptively fusion-competent sites of the myoblast plasma membrane. The present study indicates that the dynamic clustering and dispersion of lipid rafts contributes to the control of myogenic cell fusion in a novel mode of action.

Materials and methods

Cell culture

The mouse myogenic cell clone Ric10 was established from muscle satellite cells of the normal gastrocnemius muscle of an adult female ICR mouse [1,5]. Ric10 cells were plated on dishes coated with type I collagen (Sumilon, Tokyo, Japan) and cultured at 37 °C under 10% CO_2 in pmGM consisting of Dulbecco's modified Eagle's medium supplemented with 20% fetal bovine serum (FBS), 2% Ultroser G (Biosepra, Cedex-Saint-Christophe, France), and glucose (4.5 mg/ml) [1,14–16]. For induction of myogenic differentiation, the cells were plated and cultured for 24 h in pmGM, and then the medium was changed to pmDM consisting of the chemically defined medium TIS [17,18] supplemented with 2% FBS.

For induction of myosheet formation, Ric10 cells were cultured in pmDM supplemented with 24 μM forskolin (Sigma, St. Louis, MO) or 125 ng/ml CTB (Calbiochem, San Diego, CA).

For removal of cholesterol from the plasma membrane, the cells were cultured in pmDM supplemented with 5 mM methyl-β-cyclodextrin (MCD) (Sigma). To quench an ability of MCD to remove membrane cholesterol, 0.625 mM cholesterol was pre-loaded on 5 mM MCD as described [19].

For micromass culture, the dissociated single cells were cultured in pmGM at a high density of 1×10^5 cells per 100-μl spot in a 35-mm dish. After incubation for at least 2 h, 1.5 ml of pmGM was carefully added to each dish.

Transfection to establish cell clone expressing GFP-GPI

pMiw-bsr, which was derived from pMiwCAT (kindly provided by H. Kondoh, Osaka University), contains a blasticidin-resistant gene (*bsr*) under the control of a β-actin promoter and a Rous sarcoma virus enhancer. Ric10 cells (2×10^4 cells in a 35-mm dish) were transfected with 0.9 μg of pCAAG-GFP-GPI [20,21] and 0.1 μg of pMiw-bsr in the presence of 4.5 μl of FuGENE6 transfection reagent (Roche Diagnostic, Mannheim, Germany) as described [17,18,22]. Ric10-derived clones constitutively expressing GFP-GPI were selected in the presence of blasticidin S (8 μg/ml) (Funakoshi, Tokyo, Japan). One of the isolated clones, designated GSS25, was used for further analyses because it preserved robust potential for myogenic differentiation and a high level of GFP-GPI expression.

Immunofluorescence and immunocytochemical analyses

Cells were grown on collagen-coated culture dishes, then fixed, permeabilized, and processed for immunostaining as described [1,5]. Primary antibodies included mouse monoclonal antibodies to sarcomeric myosine heavy chain (MyHC) (MF20; undiluted culture supernatant) [23], M-cadherin (1: 250 dilution; BD Biosciences, San Jose, CA), β-catenin (1:500 dilution; BD), p120-catenin (1:1000 dilution; BD), N-cadherin (1:100 dilution;BD), a rabbit polyclonal antibody to GFP (1:500 dilution, Medical Biological Laboratory, Nagoya, Japan), or a goat polyclonal antibody to PKA type II subunit (1:100 dilution; Upstate, Lake Placid, NY). Secondary antibodies included biotinylated antibodies to mouse (1:1000 dilution; Jackson ImmunoResearch Laboratory, Bar Harbor, ME) or goat (1:1000 dilution; Zymed Laboratories, San Francisco, CA) immunoglobulin G, Cy3-labeled antibodies to mouse immunoglobulin G (1:1000 dilution; Jackson ImmunoReseach Laboratory) and fluorescein isothiocyanate-labeled antibodies to rabbit immunoglobulin G (1:100 dilution; Cappel Laboratories, Downington, PA). The biotinylated antibodies were detected with Alexa 488 (Molecular Probes, Eugene, OR) or horseradish peroxidase-conjugated streptavidin. The peroxidase reaction was performed with 3,3-diaminobenzidine (Sigma). Cell nuclei were stained with 2, 4-diamidino-2-phenylindole dihydrochloride *n*-hydrate (DAPI) (0.5 μg ml^{-1}, Sigma) or Mayer's hematoxylin (Wako Pure Chemicals, Osaka, Japan). Samples were visualized using an inverted microscope (model IX71; Olympus, Tokyo, Japan) and a CCD camera (DP70; Olympus). Images were post-processed using Adobe Photoshop (Adobe Systems, San Jose, CA).

Visualization of localized F-actin, GM1, and cholesterol

F-actin in cells fixed with 4% paraformaldehyde was detected by incubation of the cells for 30 min in a solution containing Alexa Fluor 546-labelled phalloidin (66 nM) (Invitrogen, San Diego, CA). For detection of GM1, cells were placed on ice and incubated for 5 min with Alexa Fluor 488-labelled CTB (1 μM) (Molecular Probes, Eugene, OR). Then the cells were fixed with 4% paraformaldehyde. To visualize the distribution of cholesterol, cells were incubated for 5 min with fluorescein-labeled poly(ethylene glycol) cholesteryl ester (fPEG-Chol) (1 μM) [24,25], and then fixed with 4% paraformaldehyde.

Immunoblotting

Sample preparation and immunoblot analysis were performed as described [18,22,26]. Immune complexes were detected by colorimetry with a BCIP/NBT detection kit (Nacalai, Kyoto, Japan).

Time-lapse recording

Cells were cultured in neutral red-depleted pmDM and placed in a humid chamber (Tokai Hit, Fujinomiya, Japan) maintained at 37 °C under 10% CO_2. Time-lapse images were taken using an inverted microscope (BZ9000; Keyence, Osaka, Japan) with a 20× Plan Apo Fluor objective lens (Nikon, Tokyo, Japan).

Quantification of muscle cell hypertrophy and lamellipodium formation

Cell quantification was done as described [5]. The distribution of myogenic cell sizes was determined by calculating the percentage

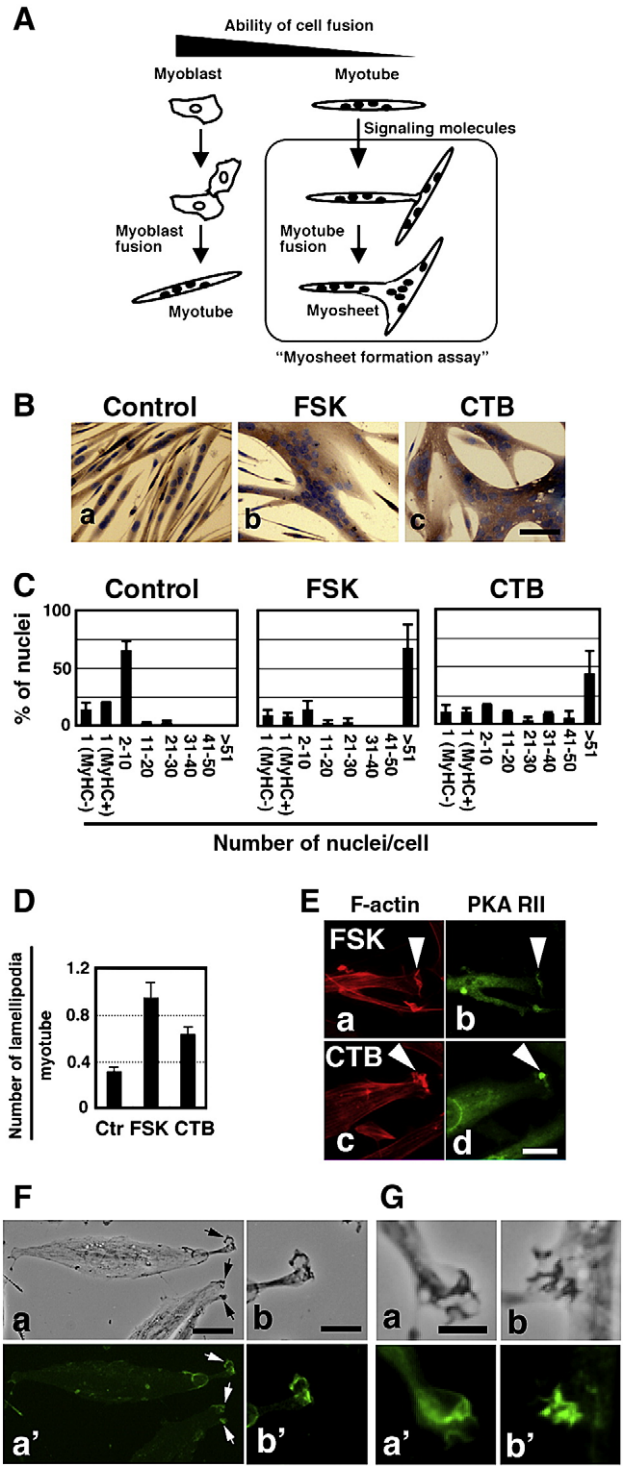

Fig. 1 – CTB induces muscle cell hypertrophy. (A) Myosheet formation assay. The ability of extracellular signaling molecules to enhance myotube fusion can be determined in myotube culture in vitro. (B) Ric10 cells (2×10^4 cells per 35-mm dish) were cultured for 36 h in pmDM (a) or in pmDM supplemented with 24 μM forskolin (b) or 125 ng/ml CTB (c). Then the cells were immunostained for MyHC. Nuclei were counterstained with Mayer's hematoxylin. Images were obtained by bright field microscopy. Scale bar: 40 μm. (C) Histograms represent the distribution of myogenic cells with different numbers of nuclei in unstimulated (left panel), forskolin-stimulated (middle panel), or CTB-stimulated (right panel) cultures after 36 h of differentiation culture. Mononucleated cells were classified to two subpopulations: one expressed MyHC (MyHC+) and the other did not (MyHC−). (D) Ric10 cells (1×10^4 cell per 35-mm dish) were cultured for 48 h in pmDM (Ctr), pmDM supplemented with 24 μM forskolin (FSK), or pmDM supplemented with CTB. Actin filaments in lamellipodia were stained with Alexa Fluor 546-labelled phalloidin. The number of lamellipodia in at least 100 myotubes per dish was counted under a phase-contrast and epifluorescence microscope. Each myotube formed 0, 1, or 2 lamellipodia at their polar ends. Averages and standard deviations of numbers of lamellipodia per myotube from three independent cultures are shown. (E) After 36 h of culture in pmDM containing forskolin (a and b) or CTB (c and d), Ric10 cells were subjected to immunostaining with anti-PKA RII antibody (RII) (b and d). Actin filaments were stained with Alexa Fluor 546-labelled phalloidin (a and c). Arrowheads represent the leading edges of lamellipodia. Images were obtained by epifluorescence microscopy. Scale bars: 20 μm. (F, G) After 36 h of culture in pmDM containing forskolin, small myotubes of Ric10 cells were subjected to staining with Alexa Fluor 488-labelled CTB (a' and b' in F), or fPEG-Chol (a' and b' in G). Arrows represent the leading edges of lamellipodia. Images were obtained by bright field (upper panels in F and G) and epifluorescence (lower panels in F and G) microscopy. Scale bars: 50 μm in (Fa), 10 μm in the others.

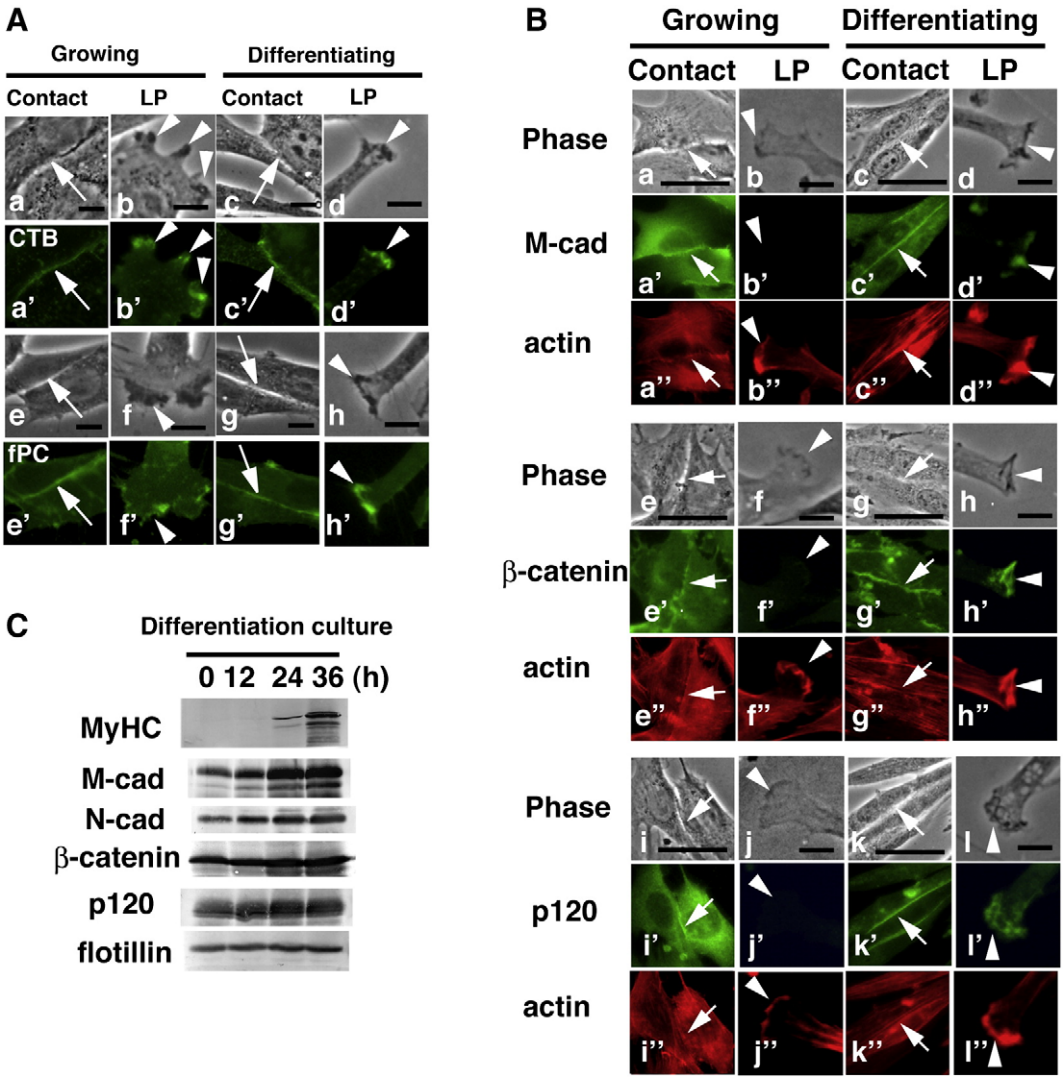

Fig. 2 – Raft markers and adhesion molecules are localized at leading edge of lamellipodia and cell–cell contacts. (A) Ric10 cells (2×10^4 cells per 35-mm dish) were cultured in pmGM for 24 h and then cultured in pmGM (a, b, e, and f) or in pmDM for 30 h (c, d, g, and h). Raft markers GM1 (a'–d') and cholesterol (e'–h') were visualized by Alexa 488-labelled CTB (CTB) and fPEG-Chol (fPC), respectively. GM1 and cholesterol were enriched in cell–cell contact regions (Contact; a, c, e and g) and lamellipodia (LP; b, d, f and h) under both growing and differentiation-inducing conditions. Arrows represent plasma membranes at cell contacts. Arrowheads represent the leading edges of lamellipodia. Images in (a–h) were obtained by phase-contrast microscopy, and those in (a'–h') were obtained by epifluorescence microscopy. Scale bars: 10 μm. (B) Ric10 cells (2×10^4 cells per 35-mm dish) were cultured for 30 h in pmDM. Then the cells were subjected to immunostaining with anti-M-cadherin antibody (a'–d'), anti-β-catenin (e'–h'), or anti-p120-catenin (p120) (i'–l'). Actin filaments were stained with Alexa Fluor 546-labelled phalloidin (a"–l"). Arrows represent plasma membranes at cell contacts. Arrowheads represent the leading edges of lamellipodia. Images in (a–l) were obtained by phase-contrast microscopy, and those in (a'–l' and a"–l") were obtained by epifluorescence microscopy. Scale bars: 10 μm. (C) Total lysates (20 μg of proteins) were prepared from cells that were cultured in pmDM for 0 h (lanes 1), 12 h (lanes 2), 24 h (lanes 3), or 36 h (lanes 4), and then subjected to immunoblot analysis for the represented proteins. Flotillin, a marker of lipid rafts, was used as a loading control.

of nuclei in myogenic cells with different numbers of nuclei in the total number of nuclei (myoblasts plus myotubes).

Fractionation of detergent-resistant membranes

Ric10 cells (1×10^5 cells/100 μl spot) were micromass cultured. A total 1×10^6 cells/10 spots were cultured in two 100-mm dishes for 24 h in pmGM and then further incubated for 12 h in pmDM. The cells were lysed in 0.2 ml of ice-cold lysis buffer (0.5% Trion X-100, 50 mM MES (pH 6.0), 50 mM NaCl, 5 mM $MgCl_2$, and 2.5 mM EGTA) containing protease inhibitor (Complete Protease Inhibitor Cocktail EDTA-free; Roche, Mannheim, Germany) for 30 min on ice. Protein concentrations in aliquots of cell lysates were determined using a BCA kit (Sigma). An aliquot of the lysate containing 319–434 μg protein was mixed with OptiPrep (Axis-Shield, London, UK) and fractionated in a 3 ml Optiprep gradient

according to manufacturer's instructions (Caveolae/Rafts Isolation Kit; Sigma). Ten fractions were collected from the top and 30 μl of each fraction was analyzed by immunoblotting. The PVDF membranes were scanned, and the signal intensity of each band was quantified using Image J software (NIH). The distribution of the protein in each fraction was determined by calculating the ratio of the signal intensity of the protein band in each fraction to the sum of the signal intensity in all fractions. Changes of protein distributions in MCD-treated cells were represented as "% Difference", which was estimated as follows: [distribution of the protein in each fraction of MCD-treated cells (%)] − [distribution of the protein in each fraction of untreated control cells (%)].

Online supplementary materials

Fig. S1 shows the expression levels of MyHC and M-cadherin in myoblasts stimulated with forskolin and CTB. Fig. S2 shows detection of M-cadherin at the leading edge of lamellipodia in differentiating myoblasts without permeabilization. Fig. S3 shows the lipid raft-dependent distributions of N-cadherin and NCAM on the leading edge of lamellipodia in differentiating myoblasts. Fig. S4 shows the distributions of adhesion molecules on the detergent-resistant membrane fractions of differentiating myoblasts. Movies 1 and 2 show the dynamic clustering and dispersion of lipid rafts at the leading edge of lamellipodia of differentiating myoblasts. Movies 3 and 4 show the dynamic clustering and dispersion of lipid rafts at the ruffling membranes of differentiating myoblasts.

Results

Cholera toxin B subunit induces muscle cell hypertrophy

Terminally differentiated multinucleated myotubes tend to lose the capacity to fuse during terminal muscle differentiation. Previously, we showed that cAMP-elevating reagents such as an adenylate cyclase activator forskolin induce cell fusion between myotubes, which give rise to a large sheet-like syncytium designated a "myosheet" [5]. To identify the key surface molecules that render an area of the plasma membrane fusion-competent, we determined the ability of extracellular signaling molecules to enhance myosheet formation in vitro (Fig. 1A). Mouse myogenic progenitor cells C2C12 or Ric10 [1,5] were stimulated with a series of growth factors, ligands, or extracellular matrices. We found that CTB induced myosheet formation in mouse myogenic cells. Ric10 cells were cultured for 36 h in pmDM supplemented with CTB. When plated at low density (2×10^4 cells per 35-mm dish), Ric10 cells gave rise to small bipolar myotubes under differentiation-inducing conditions (Fig. 1Ba). In contrast, Ric10 treated with CTB formed large syncytia that were similar to myosheets formed in forskolin-stimulated Ric10 cells (Fig. 1Bb and c). In control cultures, most myotubes contained 2 to 10 nuclei, and the maximum number of nuclei in myotubes was no more than 30 throughout the culture period (Fig. 1C left panel). In contrast, CTB- or forskolin-stimulated Ric10 cells formed extra-large myotubes containing more than 51 nuclei (Fig. 1C middle and right panels). Both the ratio of the number of nuclei in myotubes to the total number of nuclei, which is called the "fusion index", and the differentiation index, which represents the ratio of the number of nuclei in MyHC-expressing cells to the total number of nuclei, reached similar levels after 36 h of culture in unstimulated and forskolin- or CTB-stimulated Ric10 cells (Fig. 1C). In addition, expression levels of the muscle differentiation marker sarcomeric MyHC and the muscle-specific adhesion molecule M-cadherin were similar in unstimulated and forskolin- or CTB-stimulated Ric10 cells (Supplementary Fig. S1). The results imply that CTB enhances cell fusion between myotubes independently of stimulation of cell differentiation in a manner similar to forskolin.

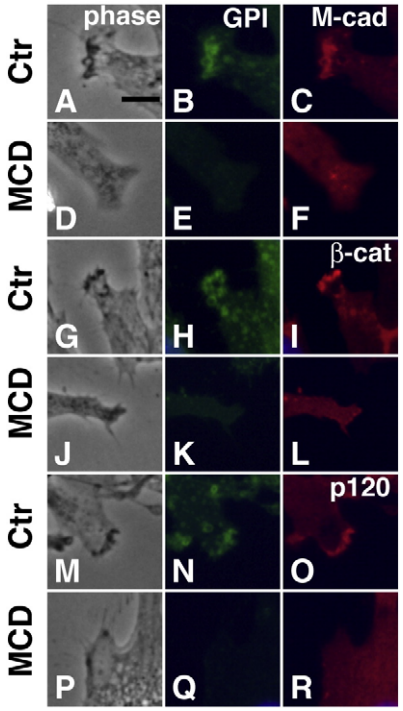

Fig. 3 – Accumulation of adhesion proteins at leading edge of lamellipodia is completely dependent on lipid raft structures. GSS25 cells, a Ric10 cell-derived clone expressing GFP-GPI, (2×10^4 cells per 35-mm dish) were cultured in pmDM for 30 h and then incubated a further 30 min in pmDM (Ctr)(A–C, G–I, and M–O) or in pmDM supplemented with 5 mM MCD (MCD) (D–F, J–L, and P–R). Lipid rafts were visualized by GFP-GPI, which was further probed with anti-GFP antibody (B, E, H, K, N and Q). M-cadherin (C and F), β-catenin (I and L), and p120-catenin (O and R) were detected with specific antibody. Images in the left panels were obtained by phase-contrast microscopy, and those in other panels were obtained by epifluorescence microscopy. Scale bars: 10 μm.

Forskolin enhanced lamellipodium formation in myotubes prior to cell fusion through activation of cyclic adenosine monophosphate-dependent protein kinase (PKA) (Fig. 1D) [5]. To determine the effects of CTB on the formation of lamellipodia in small bipolar myotubes, Ric10 cells were seeded at low density (1×10^4 cells per 35-mm dish) and cultured for 48 h in pmDM supplemented with CTB. CTB treatment significantly increased the frequency of lamellipodium formation in Ric10 myotubes, as shown in forskolin-treated Ric10 cells (Fig. 1D). Immunostaining analysis showed that the type II regulatory subunit of PKA was enriched in the leading edge of lamellipodia where F-actin was

accumulated in CTB-treated Ric10 cells (Fig. 1Ec and d), as shown in forskolin-treated Ric10 cells (Fig. 1Ea and b). Taken together with the results here, CTB is likely to enhance myotube fusion in a manner similar to forskolin.

The lipid raft marker ganglioside GM1 is a major binding target of CTB. Fluorescent dye-conjugated CTB demonstrated the presence of GM1 in the leading edge of lamellipodia of small myotubes that were stimulated with forskolin (Fig. 1F). Marked accumulation of fPEG-Chol in the leading edge of lamellipodia of forskolin-stimulated myotubes also suggests the clustering of lipid rafts (Fig. 1G) because cholesterol is well known to be enriched in lipid rafts. The results suggest that lipid rafts are involved in the capacity of lamellipodia for plasma membrane fusion.

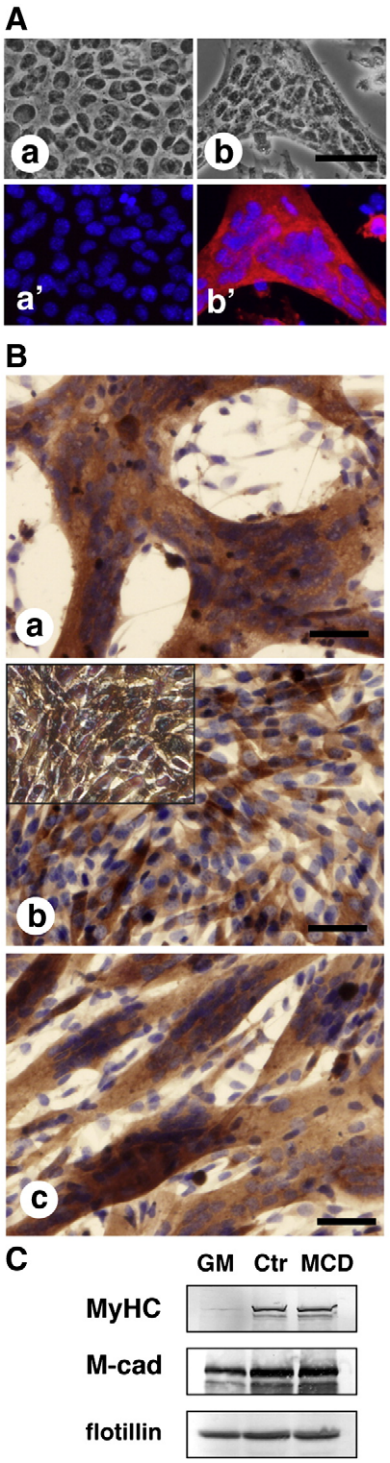

Fig. 4 – MCD prevents plasma membrane union of myogenic cells. (A) Ric10 cells (1×10^5 cells per 35-mm dish) were cultured in pmGM for 30 h and then further cultured in pmGM (a and a') or pmDM (b and b') for up to 24 h. The cells were fixed and subjected to immunostaining for MyHC (red) in (a' and b'). Cell nuclei were stained with DAPI (blue). (a') and (b') show the same areas as (a) and (b), respectively. Images were obtained by phase-contrast (a and b) and epifluorescence (a' and b') microscopy. Scale bar: 50 μm. (B) Ric10 cells (1×10^5 cells per 100 μl of spot) were cultured in micromass in pmGM for 24 h, and then further cultured in pmDM (a) or pmDM supplemented with 5 mM MCD (b) or 5 mM MCD preloaded with cholesterol (c) for up to 16 h. Then the cells were fixed and subjected to immunostaining with anti-MyHC antibody. Nuclei were counterstained with Mayer's hematoxylin. Images were obtained by bright field (a, b and c) and phase-contrast (an inlet in (b)) microscopy. The inlet in (b) shows complete inhibition of cell fusion in MCD-treated culture. Scale bar: 50 μm. (C) Ric10 cells (1×10^5 cells per 100 μl of spot) were cultured in micromass in pmGM for 24 h (lane 1) and then further cultured in pmDM (lane 2) or pmDM supplemented with 5 mM MCD (lane 3) for up to 16 h. Total cell lysates (20 μg) were subjected to immunoblot analysis for the represented proteins. Flotillin, a marker of lipid rafts, was used as a loading control.

Adhesion molecules accumulate at leading edge of lamellipodia

CTB induces lipid raft aggregation or patching [27]. The CTB-induced myosheet formation implicates the role of lipid rafts in cell fusion of mononucleated myogenic progenitor cells as well as myotubes. If this is indeed the case, lipid rafts may play a role in cell fusion exclusively under myogenic differentiation-inducing conditions because growing myogenic cells don't fuse with each other. Next, a series of experiments were done to elucidate the role of lipid rafts in cell fusion of mononucleated myogenic progenitor cells. First, the distributions of raft markers were determined in growing and differentiating myoblasts. Binding of fluorescent CTB showed that GM1 was accumulated in cell-to-cell contact regions and the leading edge of lamellipodia under both growth- and differentiation-inducing conditions (Fig. 2Aa–d). fPEG-Chol was also enriched in cell-to-cell contact regions and the leading edge of lamellipodia under both culture conditions (Fig. 2Ae–h). The results indicate that the distribution of lipid rafts is not affected by culture conditions.

Second, the distribution of M-cadherin and its associated proteins in sites of the plasma membrane in which lipid rafts clustered was determined by immunostaining analyses. M-cadherin accumulated at cell contacts in both growing and differentiating myoblasts (Fig. 2Ba and c). M-cadherin also accumulated at the leading edge of lamellipodia during differentiating culture exclusively (Fig. 2Bd) but not at the leading edge of lamellipodia in growing culture (Fig. 2Bb). An antibody against the extracellular domain of M-cadherin also recognized M-cadherin at the lamellipodia of differentiating myoblasts, the membrane of which was not

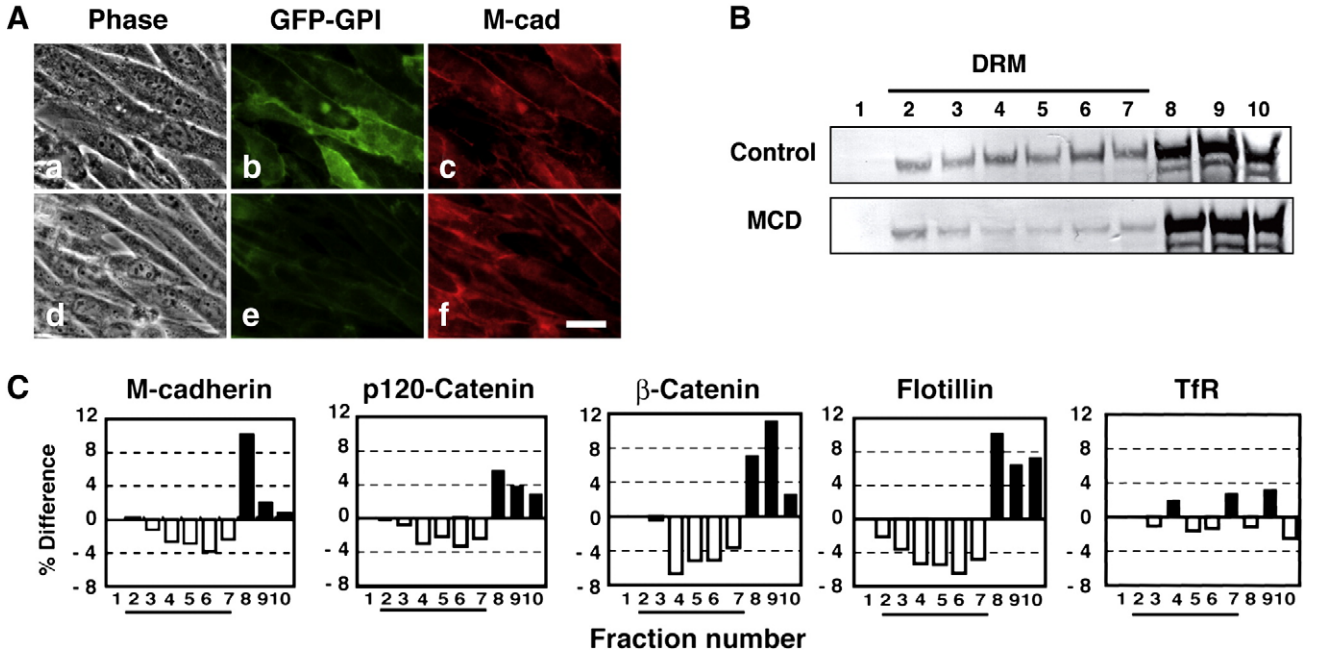

Fig. 5 – MCD impairs accumulation of adhesion proteins at lipid rafts but not adhesion of myogenic cells. (A) GSS25 cells were cultured in micromasses for 12 h in pmDM (Ctr)(a–c) or pmDM supplemented with 5 mM MCD (MCD)(d–f). The cells were subjected to immunostaining with anti-GFP (b and e) and anti-M-cadherin (c and f) antibodies. (a) and (d) show the same areas as (b and c) and (e and f), respectively. Scale bars: 25 μm. (B) The distribution of M-cadherin in each fraction (30 μl) of untreated (Control) or MCD-treated GSS25 cells (MCD) was analyzed by immunoblotting with the appropriate antibody. The line represents the detergent-resistant membrane fractions. (C) The redistribution of the adhesion proteins M-cadherin, p120-catenin, and β-catenin, in each fraction of MCD-treated cells is represented as the % difference of adhesion proteins in each fraction of control cultures. Flotillin was used as a marker of lipid raft. Transferrin receptor (TfR) was used as a marker of non-raft membrane. The lines represent the detergent-resistant membrane fractions. Similar results were obtained from more than two independent experiments. Representative data were shown.

permeabilized (Supplementary Fig. S2), implying that M-cadherin maintains a transmembrane position independent of cell contacts. β-catenin and p120-catenin, which are associated with the intracellular domain of M-cadherin, were localized at the leading edge of lamellipodia of differentiating but not growing myogenic cells, although they continuously accumulated at cell contacts (Fig. 2Be–h and i–l). The protein levels of M-cadherin increased during myogenic terminal differentiation (Fig. 2C), and might contribute to its localization at the leading edge of differentiating cells. The levels of β-catenin, p120-catenin, and N-cadherin also increased slightly during myogenesis. In addition, N-cadherin and NCAM, accumulated at the leading edge of lamellipodia of differentiating myoblasts (A. Mukai and N. Hashimoto, unpublished), although NCAM also accumulated there in growing myoblasts.

Accumulation of adhesion proteins at lamellipodia depends on lipid rafts

Differentiation culture-dependent accumulation of adhesion proteins at the leading edge of lamellipodia suggests that lipid raft structures ferry the adhesion proteins to the site. A species of Ric10 cells constitutively expressing GFP-GPI, designated GGS25, was established to visualize lipid rafts in living cells. A cholesterol-binding agent MCD removes cholesterol from the plasma membrane and disrupts lipid rafts [28]. GSS25 cells were cultured in pmDM for 30 h and then exposed to 5 mM MCD for 30 min. MCD disrupted lipid rafts and impaired the accumulation of M-cadherin, N-cadherin, NCAM, β-catenin, and p120-catenin at the leading edge of lamellipodia, resulting in their homogenous distribution throughout the whole plasma membrane (Fig. 3) (Supplementary Fig. S3). The results suggest that lipid rafts are required for the accumulation of adhesion-related proteins at the presumptively fusion-competent site of the plasma membrane in lamellipodia and play a role in cell adhesion that is prerequisite for membrane fusion.

Lipid rafts are required for plasma membrane fusion of myogenic cells

Myogenic cell fusion consists of a series of steps including cell–cell contact, recognition, adhesion, and plasma membrane breakdown/union. To assess the ability of a membrane to fuse, Ric10 cells were seeded at high cell density (1×10^5 cells per 35-mm dish). The high cell density culture allowed cell–cell contact and adhesion of Ric10 cells within a day of plating. When cultured in growth medium, Ric10 cells adhered to each other but didn't fuse during 24 h of culture after plating (Fig. 4Aa). By contrast, when the medium was switched to pmDM, mononucleated progenitor cells gave rise to multinucleated myotubes within 24 h of differentiation culture (Fig. 4Ab). The results show that cell adhesion is not sufficient for

membrane fusion, and that the plasma membrane union of mononucleated myogenic progenitor cells is highly dependent on the differentiation-inducing condition.

To determine whether lipid rafts are involved in the regulation of the plasma membrane union, Ric10 cells were cultured in micromass. Under the micromass culture condition, cell–cell contact, recognition, and adhesion were completed soon after seeding. When the medium was switched to pmDM, myoblasts gave rise to myotubes within 16 h of culture (Fig. 4Ba). In contrast, MCD-treated cells did not form multinucleated myotubes (Fig. 4Bb). In addition, the inhibition of myotube formation by MCD was rescued by prior loading of MCD with cholesterol [19,29] (Fig. 4Bc). However, in spite of the suppression of membrane fusion, MCD did not impair the expression of the myogenic differentiation marker MyHC and the muscle-specific adhesion molecule M-cadherin (Fig. 4C).

To determine the distributions of lipid rafts and M-cadherin, GGS25 cells were cultured in micromass and then treated with MCD. In control cultures, GFP-GPI and M-cadherin colocalized at the cell–cell contact regions (Fig. 5Aa–c). MCD severely disrupted lipid rafts (Fig. 5Ae). However, in contrast to the leading edge of lamellipodia, M-cadherin remained at cell contact points where lipid raft structures had broken down (Fig. 5Ad–f). In addition, MCD didn't affect the expression levels of M-cadherin (Fig. 4C). The results indicate that once cell adhesion is established in micromass culture, it can be maintained even when lipid rafts were disrupted, although lipid rafts are assumed to be required for establishing cell adhesion. Cellular fractionation experiments show that MCD disrupted lipid raft structures and that M-cadherin, β-catenin and p120-catenin were translocated from the lipid rafts to soluble fractions (Fig. 5B and C) (Supplementary Fig. S4) even though a part of lipid rafts still remained in micromass culture treated with MCD (see flotillin in Supplementary Fig. S4). However, cell adhesion did not seem to be impaired by MCD (Fig. 5Ad). Therefore, it is assumed that MCD prevents myogenic cell fusion through suppression of membrane union in micromass culture, but does not prevent the preceding steps, such as cell adhesion.

Lateral dispersion of lipid rafts from presumptive fusion sites

The present results suggest that cholesterol-enriched lipid rafts cluster at the presumptive fusion site and are required for cell adhesion and membrane fusion. However, membrane fusion takes place within the cholesterol-free areas of the myogenic cell plasma membrane [11]. The cholesterol concentration of the membrane decreases prior to membrane union because an increase in membrane fluidity is required for union. To understand this discrepancy, clustering and dispersion of lipid rafts at the leading edge of lamellipodia were observed in GSS25 cells using GFP-GPI as a raft marker. Our preliminary experiments showed that lipid rafts at the leading edge repeated the clustering-dispersion cycles quickly (Supplementary Movies 1 and 2). Therefore, the redistribution of lipid rafts during the initial contact and membrane union was visualized using GFP-GPI and sequentially observed every 60 s by time-lapse recording. Lipid raft structures remained constant at points of cell contact, and membrane fusion was not induced there even under the differentiation-inducing condition (Fig. 6A). In contrast, the leading edge of the lamellipodium fused to the opposing plasma membrane within a couple of hours after initial contact under the differentiation-inducing condition (Fig. 6B). The lamellipodium moved quickly, and lipid rafts repeatedly clustered and diffused, even after the initial contact with a fusion partner. One hour later, the lamellipodium stopped moving and lipid rafts clustered at the leading edge, which adhered to an adjacent cell (Fig. 6Bb and c). Then, prior to membrane fusion, lipid rafts were laterally dispersed from the center of the lamellipodium (Fig. 6Bd). Soon after, the lipid raft-free area of the plasma membrane started to fuse with the opposing membrane (Fig. 6Be). The results suggest that the dynamic clustering/dispersion of lipid rafts at the leading edge of lamellipodia is essential for plasma membrane fusion of myogenic

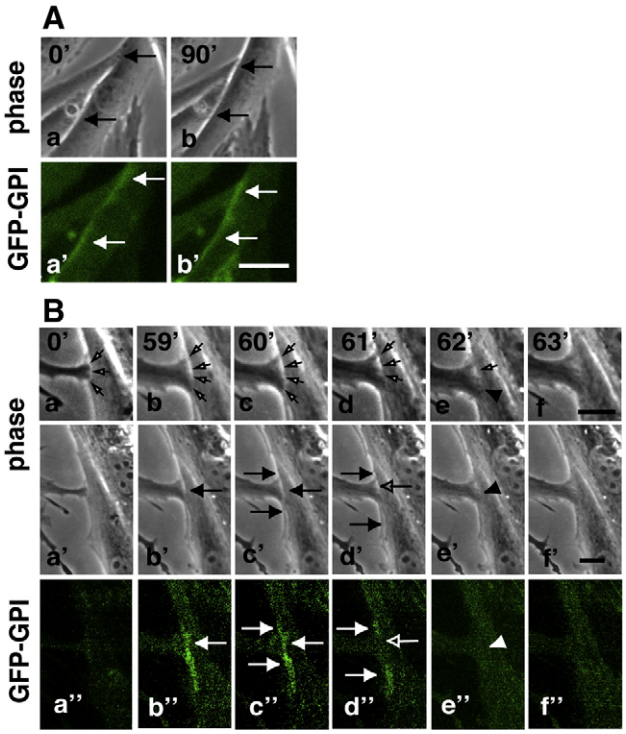

Fig. 6 – Dynamic clustering and dispersion of lipid rafts at leading edge of lamellipodia prior to membrane fusion. (A) GSS25 cells (2×10^4 cells per 35-mm dish) were cultured for 36 h in pmDM. Changes in distribution of lipid rafts were recorded by phase-contrast, epifluorescent, time-lapse microscopy. Images were obtained at the indicated time points. Arrows indicate the robust distribution of lipid raft marker GFP-GPI at cell contacts. Scale bar: 10 μm. (B) The process of cell fusion between in GSS25 culture was recorded by phase-contrast, epifluorescent, time-lapse microscopy. The lamellipodia of one myogenic cell fused to the lateral plasma membrane of another myogenic cell. Images were obtained at the indicated time points. Open arrows in (a–e) represent the cell contact site where the opposed membranes did not fuse each other yet. Arrowheads in (e, e' and e") indicate the initiation site of membrane fusion. Filled arrows in (b'–d' and b"–d") represent the areas where lipid rafts clustered. Open arrows in (d, d' and d") represent the presumptively fusion-competent site that lacks lipid rafts. Cell-to-cell contact areas in (a'–f') were enlarged in the upper panels. Scale bars: 5 μm.

cells. Similar cycling behavior of lipid rafts was also found in the ruffling membranes of myoblasts and myotubes (Supplementary Movies 3 and 4).

Lipid raft-dependent redistribution of adhesion proteins at presumptive fusion sites

Adhesion proteins were accumulated at the presumptive fusion sites in a lipid raft-dependent fashion (Fig. 3). Thus, the redistribution of adhesion complexes at the presumptive fusion sites was determined in GSS25 cells. M-cadherin, p120-catenin and β-catenin were colocalized with lipid rafts at the leading edge of lamellipodia, which adhered to an adjacent cell (Fig. 7A–D, I–L and Q–T). Then, they were removed from the center of the lamellipodium prior to membrane fusion when lipid rafts were laterally dispersed (Fig. 7E–H, M–P and U–X). The results suggest that adhesion complexes are removed from the presumptive fusion sites just prior to membrane fusion depending on the lateral dispersion of lipid rafts. The redistribution of adhesion complexes may be required for plasma membrane fusion.

Role of dynamic redistribution of lipid raft in myogenic cell fusion

Taken together with the results reported here, the process of myogenic cell fusion can be summarized as shown in Fig. 8. The clustering of lipid rafts provides a platform to which adhesion molecules are tethered, rendering the leading edge adhesion-competent (Fig. 8A, B and C). Dispersion of lipid rafts after establishing cell adhesion gives rise to cholesterol- and adhesion complex-free, fusion-competent sites of the plasma membrane (Fig. 8D, E and F). The repeated clustering/dispersion of lipid

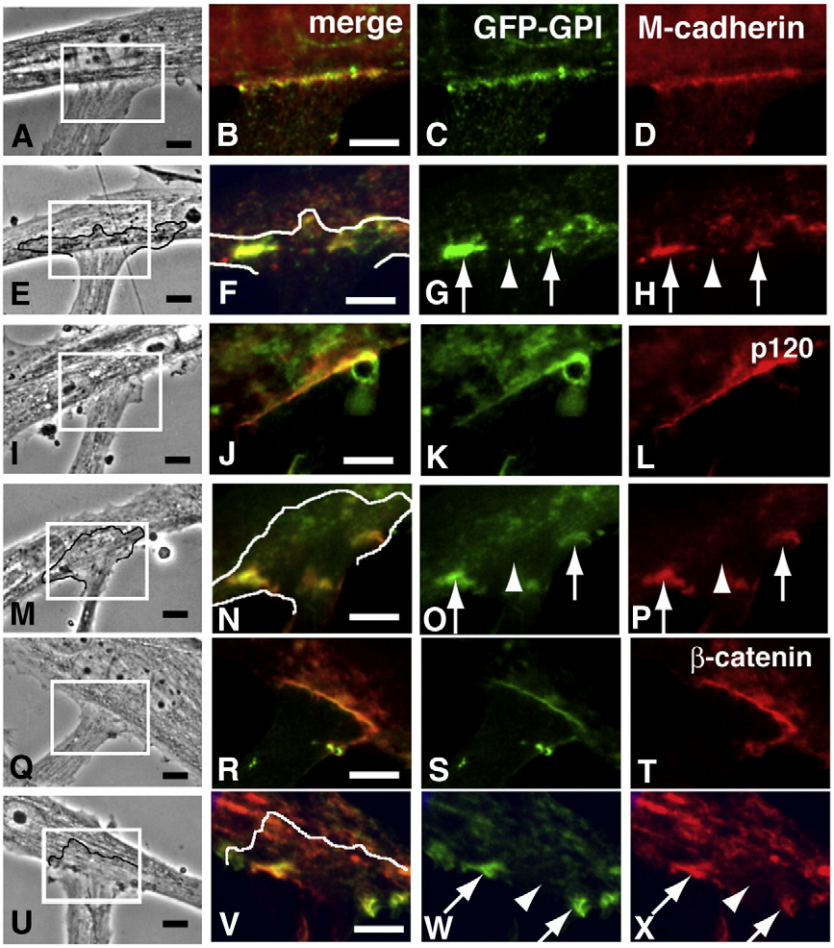

Fig. 7 – Redistribution of M-cadherin accompanies dynamic dispersion of lipid rafts at the leading edge of lamellipodium prior to membrane fusion. GGS25cells (2×10^4 cells per 35-mm dish) were cultured in pmDM for 30 h. Lipid rafts were visualized by GFP-GPI, which was further probed with an anti-GFP antibody (C, G, K, O, S and W). M-cadherin (D and H), p120-catenin (L and P) and β-catenin (T and X) were detected with specific antibodies. Images in (C and D) , (G and H), (K and L), (O and P), (S and T) and (W and X) were merged in (B), (F), (J), (N), (R) and (V) respectively. Squares in (A), (E), (I), (M), (Q) and (U) are enlarged areas in (B–D), (F–H), (J–L), (N–P), (R–T) and (V–X) respectively. Images in (A, E, I, M, Q and U) were obtained by phase-contrast microscopy, and those in other panels were obtained by epifluorescence microscopy. Line drawings in (E, F, M, N, U and V) represent the edge of the lamellipodium. Arrows represent the lipid rafts where M-cadherin, p120-catenin or β-catenin clustered. The arrow heads represent the presumptively fusion-competent site that lacks lipid rafts, M-cadherin, p120-catenin or β-catenin. In (E–H), (M–P) and (U–X), the lamellipodia went over the other cells. Scale bars: 10 μm.

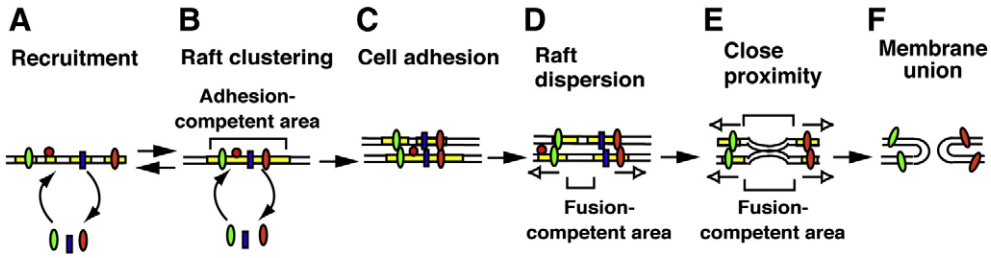

Fig. 8 – Essential role of dynamic clustering and dispersion of lipid rafts in establishing fusion competence of myogenic cells. (A and B) Lipid rafts repeat the cycle of clustering and dispersion in the leading edge of lamellipodia. The putative recruitment cycle of adhesion molecules between cytoplasm and lipid rafts is possible but has not been demonstrated. Clustering of lipid rafts induces the accumulation of adhesion molecules at the leading edge of lamellipodia and renders the area adhesion-competent (B). (C) The leading edge contacts and adheres to an adjacent cell. (D) Lateral dispersion of lipid rafts (represented by open arrows) gives rise to cholesterol- and adhesion molecule-free sites and renders the leading edge of lamellipodia fusion-competent. (E) Lateral dispersion of lipid rafts at the leading edge induces dispersion of lipid rafts on the opposing membrane (represented by open arrows). Then the opposed lipid bilayers are brought into close proximity. (F) The opposed membranes unite, and the fused area of the membranes spreads.

rafts at the leading edge of lamellipodia is essential for establishing fusion-competent sites in the plasma membrane of myogenic cells.

Discussion

We demonstrated that the dynamic clustering and dispersion of lipid rafts are required for the regulation of cell adhesion and membrane union during myogenic cell fusion. The leading edge of a lamellipodium is a presumptively fusion-competent site of the plasma membrane of myogenic cells [5]. A set of adhesion molecules accumulates at the leading edge of lamellipodia of differentiating myogenic cells in a lipid raft-dependent fashion. Lipid rafts at the leading edge of lamellipodia probably play the role of a platform tethering the adhesion molecules. The present results suggest that tethering adhesion molecules to the lipid raft in the leading edge of lamellipodia allows the molecules to function synergistically in the recognition/cell adhesion steps under a strict spatiotemporal control.

Plasma membrane breakdown/union is a final step of myogenic cell fusion. Mechanisms controlling plasma membrane breakdown/union have been studied biochemically and ultrastructurally by utilizing freeze-fracture techniques [11,12,30]. The concentration of membrane cholesterol decreases in differentiating myoblasts, producing a marked augmentation of membrane fluidity [31]. Membrane fusion takes place at discrete spots of the plasma membrane that are cholesterol-free. The decrease of membrane cholesterol is prerequisite for membrane breakdown/union because cholesterol is involved in the maintenance of plasma membrane fluidity. Therefore, dynamic redistribution of membrane cholesterol has been proposed to be a key event in plasma membrane fusion of myogenic cells.

Fusion of lipid bilayers in an aqueous environment comprises two conditions: close proximity of the membranes and destabilization of the boundary between the hydrophilic and hydrophobic portions of the bilayer [32]. We showed that dynamic lateral dispersion of lipid rafts at the leading edge of lamellipodia provided fusion-competent, cholesterol-free or low sites of the plasma membrane. Time-lapse observation reveals that the lipid raft-free sites fused to the opposing membrane of an adjacent cell. The results suggest that lateral dispersion of lipid rafts results in the reduction of membrane cholesterol at the presumptive fusion site followed by the increase of membrane fluidity and destabilization of the lipid bilayers [33].

The complex of adhesion molecules physically impairs close proximity of the opposed plasma membranes although they are relevant for cell adhesion. Lateral dispersion of lipid rafts also resulted in redistribution of adhesion complexes containing M-cadherin, β-catenin and p120-catenin that are tethered to lipid rafts. Consequently, lateral dispersion of lipid rafts at the presumptive fusion site provides adhesion complex-free spots of membrane that can be brought into close proximity. Therefore, the dynamic redistribution of lipid rafts at the presumptive fusion site is critical to render the discrete site of plasma membrane fusion-competent.

Cell adhesion and membrane fusion are sequential steps in myogenic cell fusion. However, either step requires distinct microcircumstances in the plasma membrane. To establish cell adhesion, the plasma membrane at the presumptive fusion site must contain enough cholesterol to maintain rigid lipid bilayers that hold adhesion complexes. In contrast, membrane cholesterol decreases in the same site prior to membrane fusion. In addition, adhesion complexes must be removed from the fusion site although they are relevant for cell adhesion. The mechanisms that control the rapid redistribution of membrane cholesterol and adhesion proteins during cell adhesion and membrane fusion steps have been unknown. Our data suggest that the clustering of lipid rafts provides a robust platform to tether adhesion molecules to the presumptive fusion site prior to cell contact, and that subsequent lateral dispersion of lipid rafts removes the adhesion molecules from the presumptive fusion site prior to membrane union. Furthermore, the real-time recording indicates that the opposite conditions were established in the plasma membrane of presumptive fusion sites within a couple of minutes by quick redistribution of lipid rafts. Thus, the dynamic clustering and dispersion of lipid rafts enables robust and rapid changes in plasma membrane components at the presumptive fusion site.

Lipid rafts at the leading edge of lamellipodia repeatedly clustered and diffused in the few minutes prior to cell contact, whereas those at the established cell contacts continue to be

accumulated. This dynamic behavior of lipid rafts at the leading edge is a prerequisite for their lateral dispersion prior to membrane fusion. Similar dynamic behavior of lipid rafts was also found in the ruffling membrane of myogenic cells. We observed fusion of the ruffling membrane to the opposing membrane (A. Mukai, unpublished). Therefore, we propose here that the dynamic clustering and dispersion of lipid rafts is a common feature of presumptively fusion-competent sites in the plasma membrane of myogenic cells.

Cadherins at the leading edge of lamellipodia of myogenic cells did not have partner molecules to bind to and their localization was completely independent of cell–cell contact. Detection of M-cadherin at the lamellipodia of non-permeabilized myoblasts by an antibody against its extracellular domain strongly suggests that M-cadherin normally maintains a transmembrane position independent of homophilic binding or cell contacts. The colocalization of M-cadherin, β-catenin, and p120-catenin implies that they build up an adhesion complex at the lamellipodia. The present results suggest that cadherins at the leading edge of lamellipodia are maintained as transmembrane proteins and participate in functional adhesion complexes in a cell contact-independent manner.

Membrane fusion does not take place in all areas of the closely abutted plasma membranes of myogenic cells [6] (the present study). Cell-to-cell contact induces micron-size clustering of lipid rafts and accumulation of cadherins in the plasma membrane of cell contact regions. However, membrane fusion was not induced there even under the differentiation-inducing condition. In contrast to the repeated clustering-dispersion of lipid rafts in the leading edge of lamellipodia, the cell contact-induced clustering of lipid rafts continued at cell–cell contact points after cell adhesion was established. High levels of cholesterol in the plasma membrane of cell–cell contact regions might cause rigidity, making the area of plasma membrane incapable of fusion. In addition, stable adhesion complexes might impair close proximity of the opposed plasma membranes.

Taken together with previous works, the coordination and/or balance of multiple signaling pathways is required for the regulation of the sequential steps of myogenic cell fusion. Our data indicate that the dynamic clustering and dispersion of lipid rafts plays a pivotal role in the spatiotemporal coordination of multiple adhesion molecules and catastrophic changes of plasma membrane composition that occur prior to membrane union, demonstrating that lipid rafts control myogenic cell fusion in a hitherto unappreciated mode. Further work determining the molecular pathway, which governs the clustering and dispersion of lipid rafts, will provide a novel conception of the regulation of myogenic cell fusion.

Acknowledgments

This work was supported by grants to N.H. from the Ministry of Health, Labor, and Welfare of Japan.

Appendix A. Supplementary data

Supplementary data associated with this article can be found, in the online version, at doi:10.1016/j.yexcr.2009.07.010.

REFERENCES

[1] M.R. Wada, M. Inagawa-Ogashiwa, S. Shimizu, S. Yasumoto, N. Hashimoto, Generation of different fates from multipotent muscle stem cells, Development 129 (2002) 2987–2995.
[2] M.J. Wakelam, The fusion of myoblasts, Biochem. J. 228 (1985) 1–12.
[3] K.A. Knudsen, L. Smith, S. McElwee, Involvement of cell surface phosphatidylinositol-anchored glycoproteins in cell–cell adhesion of chick embryo myoblasts, J. Cell Biol. 109 (1989) 1779–1786.
[4] E.H. Chen, E.N. Olson, Towards a molecular pathway for myoblast fusion in Drosophila, Trends Cell Biol. 14 (2004) 452–460.
[5] A. Mukai, N. Hashimoto, Localized cyclic AMP-dependent protein kinase activity is required for myogenic cell fusion, Exp. Cell Res. 314 (2008) 387–397.
[6] G. Fumagalli, A. Brigonzi, T. Tachikawa, F. Clementi, Rat myoblast fusion: morphological study of membrane apposition, fusion, and fission during controlled myogenesis in vitro, J. Ultrastruct. Res. 75 (1981) 112–125.
[7] I. Tachibana, M.E. Hemler, Role of transmembrane 4 superfamily (TM4SF) proteins CD9 and CD81 in muscle cell fusion and myotube maintenance, J. Cell Biol. 146 (1999) 893–904.
[8] R.S. Krauss, F. Cole, U. Gaio, G. Takaesu, W. Zhang, J.S. Kang, Close encounters: regulation of vertebrate skeletal myogenesis by cell–cell contact, J. Cell Sci. 118 (2005) 2355–2362.
[9] V. Horsley, G.K. Pavlath, Forming a multinucleated cell: molecules that regulate myoblast fusion, Cells Tissues Organs 176 (2004) 67–78.
[10] J. Prives, M. Shinitzky, Increased membrane fluidity precedes fusion of muscle cells, Nature 268 (1977) 761–763.
[11] T. Sekiya, T. Takenawa, Y. Nozawa, Reorganization of membrane cholesterol during membrane fusion in myogenesis in vitro: a study using the filipin–cholesterol complex, Cell Struct. Funct. 9 (1984) 143–155.
[12] M. Nakanishi, E. Hirayama, J. Kim, Characterisation of myogenic cell membrane: II. Dynamic changes in membrane lipids during the differentiation of mouse C2 myoblast cells, Cell Biol. Int. 25 (2001) 971–979.
[13] R.B. Cornell, S.M. Nissley, A.F. Horwitz, Cholesterol availability modulates myoblast fusion, J. Cell Biol. 86 (1980) 820–824.
[14] N. Hashimoto, T. Murase, S. Kondo, A. Okuda, M. Inagawa-Ogashiwa, Muscle reconstitution by muscle satellite cell descendants with stem cell-like properties, Development 131 (2004) 5481–5490.
[15] N. Hashimoto, T. Kiyono, M.R. Wada, R. Umeda, Y. Goto, I. Nonaka, S. Shimizu, S. Yasumoto, M. Inagawa-Ogashiwa, Osteogenic properties of human myogenic progenitor cells, Mech. Dev. 125 (2008) 257–269.
[16] N. Hashimoto, T. Kiyono, M.R. Wada, S. Shimizu, S. Yasumoto, M. Inagawa, Immortalization of human myogenic progenitor cell clone retaining multipotentiality, Biochem. Biophys. Res. Commun. 348 (2006) 1383–1388.
[17] N. Hashimoto, M. Ogashiwa, Isolation of a differentiation-defective myoblastic cell line, INC-2, expressing muscle LIM protein under differentiation-inducing conditions, Dev. Growth Differ. 39 (1997) 363–372.
[18] N. Hashimoto, M. Ogashiwa, S. Iwashita, Role of tyrosine kinase in the regulation of myogenin expression, Eur. J. Biochem. 227 (1995) 379–387.
[19] A.E. Christian, M.P. Haynes, M.C. Phillips, G.H. Rothblat, Use of cyclodextrins for manipulating cellular cholesterol content, J. Lipid Res. 38 (1997) 2264–2272.
[20] G. Kondoh, Development of glycosylphosphatidylinositol-anchored enhanced green fluorescent protein. One-step visualization of GPI fate in global tissues and ubiquitous cell surface marking, Methods Mol. Biol. (Clifton, N.J 183 (2002) 215–224.

[21] J.M. Rhee, M.K. Pirity, C.S. Lackan, J.Z. Long, G. Kondoh, J. Takeda, A.K. Hadjantonakis, In vivo imaging and differential localization of lipid-modified GFP-variant fusions in embryonic stem cells and mice, Genesis 44 (2006) 202–218.
[22] N. Hashimoto, M. Ogashiwa, E. Okumura, T. Endo, S. Iwashita, T. Kishimoto, Phosphorylation of a proline-directed kinase motif is responsible for structural changes in myogenin, FEBS Lett. 352 (1994) 236–242.
[23] D. Bader, T. Masaki, D.A. Fischman, Immunochemical analysis of myosin heavy chain during avian myogenesis in vivo and in vitro, J. Cell Biol. 95 (1982) 763–770.
[24] R. Ishitsuka, S.B. Sato, T. Kobayashi, Imaging lipid rafts, J. Biochem. 137 (2005) 249–254.
[25] S.B. Sato, K. Ishii, A. Makino, K. Iwabuchi, A. Yamaji-Hasegawa, Y. Senoh, I. Nagaoka, H. Sakuraba, T. Kobayashi, Distribution and transport of cholesterol-rich membrane domains monitored by a membrane-impermeant fluorescent polyethylene glycol-derivatized cholesterol, J. Biol. Chem. 279 (2004) 23790–23796.
[26] H. Hirano, T. Watanabe, Microsequencing of proteins electrotransferred onto immobilizing matrices from polyacrylamide gel electrophoresis: application to an insoluble protein, Electrophoresis 11 (1990) 573–580.
[27] A.M. Fra, E. Williamson, K. Simons, R.G. Parton, Detergent-insoluble glycolipid microdomains in lymphocytes in the absence of caveolae, J. Biol. Chem. 269 (1994) 30745–30748.
[28] L.J. Pike, J.M. Miller, Cholesterol depletion delocalizes phosphatidylinositol bisphosphate and inhibits hormone-stimulated phosphatidylinositol turnover, J. Biol. Chem. 273 (1998) 22298–22304.
[29] A.E. Christian, H.S. Byun, N. Zhong, M. Wanunu, T. Marti, A. Furer, F. Diederich, R. Bittman, G.H. Rothblat, Comparison of the capacity of beta-cyclodextrin derivatives and cyclophanes to shuttle cholesterol between cells and serum lipoproteins, J. Lipid Res. 40 (1999) 1475–1482.
[30] N. Kalderon, N.B. Gilula, Membrane events involved in myoblast fusion, J. Cell Biol. 81 (1979) 411–425.
[31] P.L. Yeagle, Lanosterol and cholesterol have different effects on phospholipid acyl chain ordering, Biochim. Biophys. Acta 815 (1985) 33–36.
[32] R. Jahn, T. Lang, T.C. Sudhof, Membrane fusion, Cell 112 (2003) 519–533.
[33] S.W. Chiu, E. Jakobsson, R.J. Mashl, H.L. Scott, Cholesterol-induced modifications in lipid bilayers: a simulation study, Biophys. J 83 (2002) 1842–1853.